JOURNAL OF EXPERIMENTAL AND THEORETICAL PHYSICS, 2024, Vol. 165, No. 6, pp. 765–774

ATOMS, MOLECULES, OPTICS

ROLE OF NEPHELAUXETIC EFFECT FOR Fe^{2+} ION IN ZINC SELENIDE AND CADMIUM TELLURIDE MATRICES

© 2024 V. S. Krivobok[a, b*], D. F. Aminev[a], D. A. Zazymkina[a], V. V. Ushakov[a], A. A. Narych[a], V. I. Kozlovsky[a], Yu. V. Korostelin[a]

[a] Lebedev Physical Institute of Russian Academy of Sciences 119991, Moscow, Russia
[b] National Research University MPTI 141701, Dolgoprudny, Moscow region, Russia
*e-mail: larionov.nickolay@gmail.com

Received September 12, 2023
Revised January 23, 2024
Accepted January 29, 2024

Abstract. For the electronic subsystem of transition metal ions embedded in a crystal lattice or formed a complex with ligands, an effective decrease in interelectron repulsion is observed compared to free ions, which in modern literature is referred to as the nephelauxetic effect. In this work, we study the role of the nephelauxetic effect in the Fe^{2+} ions electronic spectrum formation in CdTe and ZnSe matrices. Experimental assessment of the corresponding corrections was carried out based on the analysis of two transitions – the well-known $^5T_2(^5D) \rightarrow {}^5E(^5D)$, enabling us to record the magnitude of the crystal field, and the less studied $^3T_1(^3H) \rightarrow {}^5E(^5D)$. The discovery of the zero-phonon line of this transition in CdTe:Fe enabled us to compare the two luminescent systems properties and demonstrate that for the Fe^{2+} ion in CdTe the nephelauxetic effect role increases noticeably. Based on the experimental data obtained in combination with calculations within crystal field theory, we have refined the values of the Racah parameters for Fe^{2+} ions in CdTe and ZnSe matrices. The role of the nephelauxetic effect for Fe^{2+} ions in two matrices similar in structure is important both for practical problems related to IR laser systems improvement, and for resolving some fundamental questions of quantum chemistry.

Keywords: *transition metal ions, crystal lattice, crystal field, nephelauxetic effect, CdTe, ZnSe*

DOI: 10.31857/S004445102406e014

1. INTRODUCTION

Group II-VI semiconductors with cubic structure, doped with transition elements, are widely used in the development of tunable [1] and pulsed [2] lasers in the mid-IR range. Further progress in laser technologies aimed at improving existing laser systems [3, 4] or developing new approaches for laser generation [5] requires a more detailed understanding of the mechanisms of electronic spectrum formation of transition element ions in crystalline matrices. Among them, the greatest attention is paid to iron and chromium [6–8]. A consistent solution to this problem could rely on modern *ab-initio* calculations, which allow determining not only the structure and electronic spectrum of luminescent centers but also studying possible scenarios of their formation [9]. Nevertheless, at present, the capabilities of this approach are often quite limited due to the fact that for embedded transition element ions, both the correlation of interelectron motion and the existence of a large number of alternative electronic configurations contributing to the total electron density have a significant influence [10]. In this context, much attention is paid to discussing many-electron corrections within the crystal field theory, in particular, the role of the so-called nephelauxetic effect is discussed [11,12].

From the crystal field theory perspective, the nephelauxetic effect manifests as an effective reduction in Racah parameters (*B, C*), determined by the structure of electron shells, during the transition from a free ion to an ion embedded in the crystal lattice [12]. This tendency can be interpreted as an effective reduction in electron repulsion. In other words, in the presence of surroundings, a correction arises due to many-electron effects, whose physical meaning can be

qualitatively described as delocalization of single-electron orbitals and interaction of center electrons with the surroundings. Accordingly, experimental study of the nephelauxetic effect allows not only to refine the parameters of the electronic spectrum of the radiative center but also to provide some quantitative assessment of the role of many-electron motion correlation arising due to the presence of ligands. The latter circumstance is of considerable interest, particularly for establishing the accuracy of actively developing theoretical approaches [13], combining the convenience of formulation inherent in ligand field theory [14] with high-precision quantum chemistry methods [15,16], allowing for a self-consistent description of correlation effects and contributions from spin-orbital and spin-spin interactions.

Despite active study of the nephelauxetic effect for a number of chemical compounds [11, 17], its role remains poorly understood for transition element ions in crystal matrices, including the practically important case of II-VI group semiconductors with cubic structure. Experimental studies of materials in this group are complicated by the fact that spectroscopic information about several (at least two) transitions involving different electron shells becomes necessary. This feature is determined by the fact that to fix the nephelauxetic effect within crystal field theory, it is necessary to determine both the crystal field magnitude (Dq) and the exact values of Racah parameters (*B, C*). The difference of these parameters from values characteristic of the free ion will determine the role of the nephelauxetic effect.

Recently, for the quantitative description of the nephelauxetic effect, the parameter [11] has been used

$$b_1 = \sqrt{\left(\frac{B}{B_0}\right)^2 + \left(\frac{C}{C_0}\right)^2}, \quad (1)$$

where *B, C* are the Racah parameters for the ion in the crystal lattice, and B_0, C_0 are the Racah parameters for the free ion. It is considered that at $\beta_1 \sim 1$ the role of the nephelauxetic effect is secondary and becomes significant if β_1 is notably less than unity [12]. In the case of cubic II-VI semiconductors, one of the promising systems for investigating the nephelauxetic effect is iron ions in zinc selenide [18, 19]. This is due to the fact that for the optically active ion Fe^{2+} in ZnSe, at least two different transitions with well-studied fine structure are known: $^5T_2(^5D) \rightarrow {}^5E\,(^5D)$ [19. 20] and $^3T_1(^3H) \rightarrow {}^5T_2(^5D$ [21]. The first transition allows determining the role of the crystal field, while the second one helps determine the range of permissible Racah parameters and evaluate the role of the nephelauxetic effect.

Along with the well-known ZnSe:Fe, interest is drawn to a system with similar properties CdTe:Fe, which also has a cubic lattice but is characterized by a larger lattice constant, smaller value of parameter *Dq* and, apparently, more significant role of many-electron effects. The latter is determined by the fact that the matrix components Cd and Te are significantly heavier than Zn and Se [22]. For CdTe:Fe the fine structure of the transition $^5T_2(^5D) \rightarrow {}^5E\,(^5D)$ was studied in [23]; the transition $^3T_1(^3H) \rightarrow {}^5E(^5D)$ in this system has not been previously studied.

In this work, based on low-temperature photoluminescence measurements, we identified the transition $^3T_1(^3H) \rightarrow {}^5E(^5D)$ for the CdTe:Fe system. The obtained data allowed us to experimentally determine the value of parameter for this system and experimentally demonstrate the different roles of many-electron corrections, which determine the nephelauxetic effect for the inner shells of the ion Fe^{2-}, in CdTe and ZnSe matrices. The evaluation of the nephelauxetic effect obtained in this work can help not only in the development of IR laser systems but also in resolving some general issues related to many-electron effects in quantum mechanical calculations.

2. MATERIALS AND EXPERIMENTAL METHODOLOGY

For the research, polycrystalline ZnSe samples were selected, doped by Fe^{2+} thermal diffusion method, which demonstrated laser generation parameters close to record values [24]. These samples in the form of parallelepipeds were cut from a polycrystalline druse with uniform microstructure. Then, an iron film was deposited on the sample surface, and the samples were annealed in Ar atmosphere at temperature 1000–1100°C for 240 hours. For luminescence measurements, the faces of parallelepipeds located perpendicular to the surface on which the iron film was deposited were used. Along these faces, a notable gradient of dopant

iron concentration was observed [25]. Structural and optical characterization of selected samples ZnSe:Fe are described in work [26].

The laser-quality CdTe crystal doped with iron was grown at LPI using an original method [27]. The methodology is based on vapor phase transport of impurities in He atmosphere during free crystal growth. The main features of the technology are the use of two separate sources – polycrystalline II-IV material and impurity, as well as individual control of the flow rate of II-IV materials and doping impurity. The studied crystal was cut from a boule grown in He atmosphere at 1250 K. During furnace cooling, the boule was annealed for 24 hours at 1080 K. The concentration of iron ions was $4 \cdot 10^{18}$ cm^{-3}.

Low-temperature photoluminescence (PL) measurements of the samples were conducted in a wide spectral range from 0.9 to 5.5 μm (1.4–0.22 eV). For measuring spectra in the near-IR range up to 1.1 μm, a setup based on an Acton monochromator (Princeton Instruments) with a cooled silicon array was used. For operation at longer wavelengths, a setup based on a modernized IKS-31 monochromator with interchangeable diffraction gratings was used. The detection scheme employed various detectors, providing maximum sensitivity in their respective ranges. In the spectral region of 1–1.7 μm, a Hamamatsu H10330B-75 photomultiplier tube operating in photon counting mode was used for signal detection. In the 1.1–2.4 μm range, a cooled InGaAs photodiode with a transimpedance preamplifier (with cooled resistance) was used. In the mid-infrared range, a cooled MCT D313 detector was employed. For detecting the photoresponse of the InGaAs photodiode and MCT detector, we used synchronous detection implemented with a Princeton Instruments SR 830 lock-in amplifier.

To excite PL transitions from level $^3T_1(^3H)$ in ZnSe:Fe, the second harmonic of a solid-state Nd:YAG laser with a wavelength of 532 nm was used. Such excitation effectively populates level $^3T_1(^3H)$ [21]. Also, with such excitation, the population of level $^5T_2(^5D)$ will be determined $^3T_1(^3H) \rightarrow {}^5T_2(^5D)$ by transition $^5T_2(^5D) \rightarrow {}^5E(^5D)$, and the $^5T_2(^5D) \rightarrow {}^5E(^5D)$ intensity of PL line will be relatively low. Therefore, for exciting the PL transition $^3T_1(^3H) \rightarrow {}^5E(^5D)$, it is more effective to use a laser with photon energy lower than the transition energy. We used a semiconductor InGaAs laser with an excitation wavelength of 995 nm and power of 200 mW. The same laser was used to excite the main PL transition in the CdTe:Fe sample. To excite luminescence from higher-lying states, a semiconductor InGaAl laser with a radiation wavelength of 660 nm was used. This laser implements the possibility of controlling radiation using an external signal. This allows, using a pulse generator, to implement pulsed excitation of the sample and thus measure the luminescence kinetics. To control the 660 nm semiconductor laser, we used a G5-72 pulse generator. In the vast majority of cases, a pulse duration of 200 μs and a pulse repetition rate of 480 Hz were selected. This mode was chosen to register relatively long-term PL decays characteristic of intracenter transitions. The pulse front width did not exceed 100 ns, which is quite sufficient for measuring relatively slow luminescence kinetics Fe^{2-} at helium temperatures.

3. LOW-TEMPERATURE LUMINESCENCE Fe^{2+} IN CdTe AND ZnSe

Fragments of low-temperature photoluminescence spectra of the studied samples, demonstrating intracenter transitions Fe^{2+} in CdTe and ZnSe, are presented in Fig. 1. Free iron ion Fe^{2+} has configuration d^6 with the ground state being ^5D, and the first excited state – ^3H. In this work, the spectrum of ions Fe^{2+}, substituting Zn(Cd) in the lattice ZnSe(CdTe) is discussed. In this case, the impurity is in a tetrahedral field, which causes splitting of the initial levels, see Fig. 2. From crystal field theory, confirmed by experimental studies of the electronic spectrum, see, for example, [19], it follows that when considering only the electric field, the ground state ^5D splits into two terms, ^5E and $^5T_2$, while the excited term splits into three levels, $^3H \rightarrow {}^3T_1, {}^3E, {}^3T_2$. The transition between the lower levels $^5T_2(^5D) \rightarrow {}^5E(^5D)$, is well studied. Both for CdTe:Fe [23] and for ZnSe [19], a series of phonon-free lines is resolved, which allows quite accurate determination of the energy shift between levels ^5E and $^5T_2$.

From early works for ZnSe:Fe a broad emission band with a maximum around 980 nm is known [18]. Experiments with optical detection of magnetic resonance unambiguously indicate the connection of this band with the transition of $^3T_1(^3H) \rightarrow {}^5E(^5D)$ ion Fe^{2+} [18]. Recently, the use of low temperatures combined with high-quality ZnSe:Fe crystals made it possible to register six phononless components of

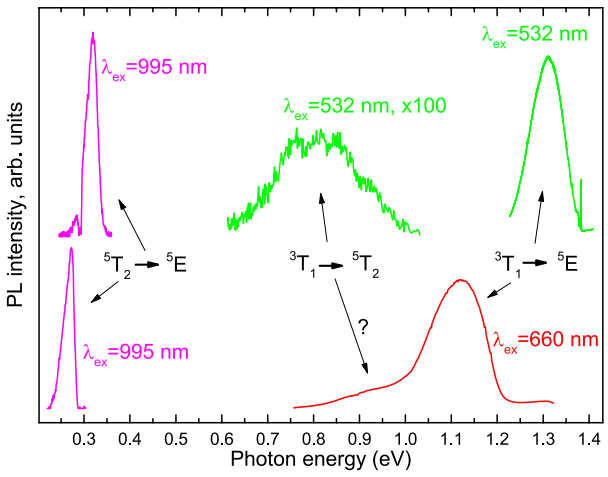

Fig. 1. Overview spectra of low-temperature photoluminescence for ions Fe^{2+} in ZnSe crystals (top) and CdTe (bottom) at a temperature of 7 K. The excitation wavelengths used are shown in the figure

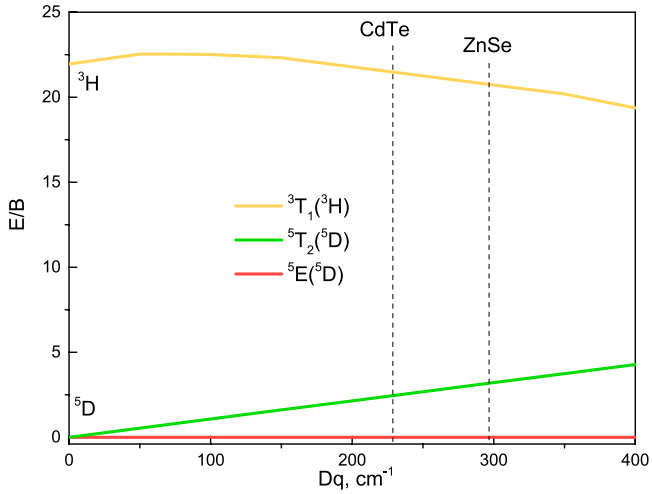

Fig. 2. Energy splitting scheme of ^3H- and ^5D- levels Fe^{2+} in a tetrahedral field (Tanabe-Sugano diagram). Vertical dashed lines correspond to the parameter values Dq for CdTe and ZnSe

the fine structure for the transition $^3T_1(^3H) \rightarrow {}^5E(^5D)$, each with a width not exceeding 0.3 meV [28]. The very presence of these components excludes a significant role of non-adiabatic effects, their number indicates tetrahedral coordination of the ion Fe^{2+}, and the energy position provides the possibility of more or less correct restoration of the Racah parameters in the ZnSe matrix. In turn, the transition $^3T_1(^3H) \rightarrow {}^5T_2(^5D)$ to the first excited sublevel was discussed in works [21,28]. The position of the blue boundary for the corresponding emission line agrees with the electronic spectrum structure derived from the spectroscopy of transitions $^3T_1(^3H) \rightarrow {}^5E(^5D)$ and $^5T_2(^5D) \rightarrow {}^5E(^5D)$. Characteristic luminescence signal decay times for transitions $^3T_1(^3H) \rightarrow {}^5E(^5D)$ and $^3T_1(^3H) \rightarrow {}^5T_2(^5D)$, determined by relaxation from state $^3T_1$ (^3H), are on the order of hundreds of microseconds [29].

For ZnSe crystals studied in this work, the luminescence spectrum corresponding to the transition $^3T_1(^3H) \rightarrow {}^5T_2(^5D)$ is shown in the center of the upper part of Fig. 1. The fine structure of the spectrum in the region corresponding to the phononless components of the transition $^3T_1(^3H) \rightarrow {}^5E(^5D)$ is shown separately in Fig. 3. The presence of several phononless peaks in the 1.379–1.387 eV region is determined by the splitting of states $^3T_1$ (^3H) and $^5E(^5D)$ due to first- and second-order spin-orbit interaction [28]. The spectral positions of the phononless lines are systematized in Table 1.

Unlike ZnSe, only the transition $^5T_2(^5D) \rightarrow {}^5E(^5D)$ was previously confidently registered for cadmium telluride. The fine structure of this transition indicates that, as in ZnSe, the coordination of the ion is close to tetrahedral. Consequently, the long-wavelength shift of the transition $^5T_2(^5D) \rightarrow {}^5E(^5D)$ [23] in CdTe compared to ZnSe is determined by the decrease in crystal field splitting (parameter D_q). For the studied CdTe:Fe crystals, the emission line corresponding to the transition $^5T_2(^5D) \rightarrow {}^5E(^5D)$ is shown in Fig. 1 bottom left.

In work [30], the emergence of new emission bands with emission maxima of 1.13 and 1.03 eV after iron implantation into CdTe and subsequent annealing is mentioned. This work also provides an estimate of emission decay time of 30 μs, which allows concluding that these bands are related to intracenter transitions of iron ions. However, no assumptions about the nature of the corresponding center were made in [30].

As seen in Fig. 1, in the studied crystals CdTe:Fe the emission band 1.2–0.75 eV has a complex shape, and it can be assumed that it is formed by the superposition of two bands – a more intense one with a maximum at 1.1 eV and a less intense one with a maximum around 0.9 eV. This assumption is based on the analogy with the emission spectrum Fe^{2+} in ZnSe, see the upper part of Fig. 1. However, this

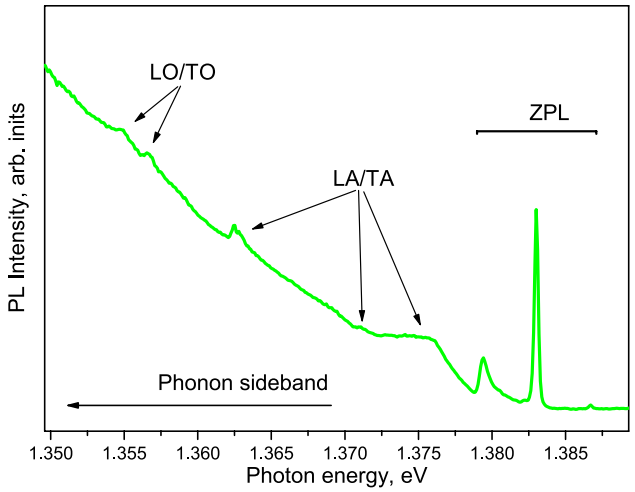

Fig. 3. Fine structure of the emission spectrum for crystal ZnSe:Fe in the zero-phonon line (ZPL) transition region $^3T_1(^3H) \rightarrow {}^5E(^5D)$ at a temperature of 5K. For PL excitation, radiation with a wavelength of 532 nm is used. LO/TO and LA/TA denote phonon replicas involving optical and acoustic phonons, respectively

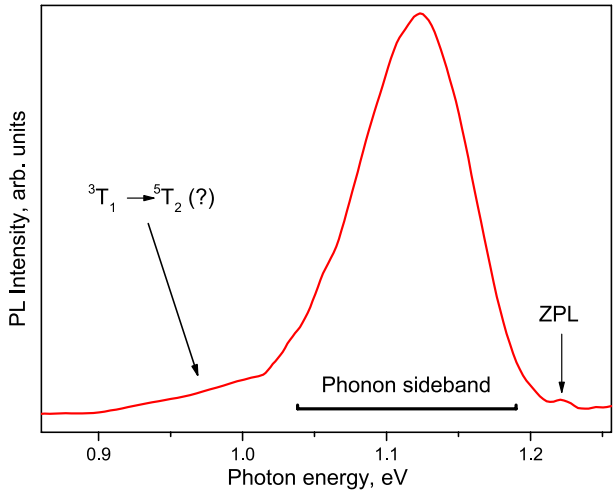

Fig. 4. Photoluminescence spectrum CdTe:Fe, recorded under pulsed excitation conditions at a temperature of 7 K. The delay relative to the end of the exciting laser pulse is 1.4 ms. The zero-phonon transition (ZPL) is located around 1.22 eV

spectral range may be overlapped by the emission of CdTe structural defects, see, for example, [31]; besides that, a contribution to the emission from iron ions in a different charge state is possible.

Unlike intra-center luminescence, conventional impurity-defect emission in semiconductors with a direct fundamental absorption edge is characterized by nano- or microsecond decay times. Therefore, to separate the luminescent background, we conducted time-resolved PL measurements. An example of an emission spectrum obtained at relatively long delay times of about 1.4 ms is shown in Fig. 4. It can be seen that this spectrum shows the main band with a maximum at 1.1 eV, a long-wavelength feature around 0.9 eV, and a weak short-wavelength component with a maximum at 1.22 eV. Based on the relatively long decay times, it can be stated that all these components represent intra-center PL.

To evaluate the nephelauxetic effect, as in the case of ZnSe:Fe, the spectral position of the zero-phonon transition (transitions) is of greatest interest. In the case of the PL spectrum in Fig. 4, the narrow component around 1.22 eV is obviously the main candidate for the zero- phonon transition. As in the case of ZnSe (Fig. 3), this line may have a fine structure that is not resolved in our experiments. To confirm this interpretation, we measured the luminescence kinetics of the 1.1 eV band and the narrow component at 7 K. The measurement results are illustrated in Fig. 5 (upper panel) (PL rise) and Fig. 5 (lower panel) (PL quenching). As can be seen in these figures, similar characteristics of signal rise and quenching are observed, which confirms that the narrow line at 1.22 eV and the broad band at 1.1 eV belong to the same luminescent system. Thus, it can be stated that the 1.22 eV peak is indeed a zero-phonon transition, and the 1.1 eV band arises from interaction with the phonon subsystem.

In CdTe crystals studied in this work, the presence of optically active iron ions Fe^{2+} is confirmed by intense luminescence corresponding to the transition $^5T_2(^5D) \rightarrow {}^5E(^5D)$, see Fig. 1. Nevertheless, Fe^{3+} ions could be a possible alternative candidate for the discussed luminescent system in CdTe. As estimates show (see Appendix), the first excited state for the ion is located around 2 eV. This is significantly higher than the spectral position of the bands in Fig. 4 (about 1.1-1.2 eV). Furthermore, in the experiments described above, we used optical excitation with quantum energy exceeding the fundamental absorption edge of CdTe. In this case, the exciting radiation is absorbed in a thin near-surface layer, and direct (intracenter) excitation of Fe^{3+} is unlikely due to the small cross-section value for the corresponding process. The most efficient excitation mechanism apparently consists of capturing a photoexcited electron by the Fe^{3+} ion and then relaxation into one of the excited states of

Table 1. Energy values of transitions observed in the experiment for ZnSe:Fe and CdTe:Fe (values given in cm^{-1})

	$^5T_2(^5D) \rightarrow {}^5E(^5D)$	$^3T_1(^3H) \rightarrow {}^5T_2(^5D)$	$^3T_1(^3H) \rightarrow {}^5E(^5D)$
ZnSe:Fe	2700-2950	7140	11155
CdTe:Fe	2197	6250	8695

the Fe^{2+} ion [21]. The Fe^{3+} ion in the CdTe lattice forms a Coulomb potential similar to a hydrogen-like donor in CdTe (properties of hydrogen-like donors in CdTe are described, in particular, in work [32]). Therefore, at helium temperatures, efficient electron capture should be expected with subsequent formation of weakly bound (hydrogen-like) states.

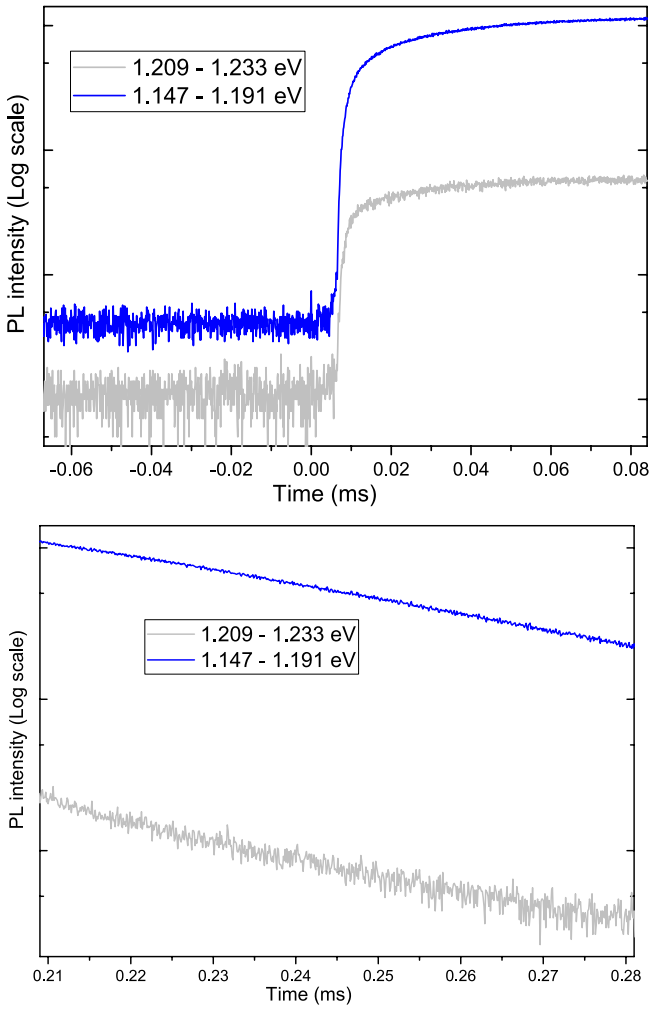

Fig. 5. The kinetics of rise (upper panel) and decay (lower panel) of the photoluminescence signal, recorded in two different spectral regions under excitation of the CdTe:Fe crystal with rectangular pulses. The first region (gray curves) corresponds to the zero-phonon (ZPL) transition in Fig. 4, the second region to a fragment of the broad band around 1.1 eV. Temperature 5 K, laser excitation wavelength 660 nm

At the same time, the Fe^{2+} ion does not form a long-range attractive potential for holes, so the process where a hole is captured by the Fe^{2+} ion with subsequent formation of the Fe^{3+} ion in anexcited state seems unlikely.

The paper [30] mentions the emergence of new emission bands with maxima 1.13 and 1.03 eV, after implantation of iron in CdTe and subsequent annealing. iron in CdTe and subsequent annealing. In this work, an estimate of the of the radiation attenuation time of 30 μs, which allows us to conclude that these bands are related with intra-centre transitions of iron ions. However, no assumptions were made in [30] on the nature of the corresponding centre.

Thus, under experimental conditions, when excited above the fundamental absorption edge, one should expect intracentral luminescence specifically from ions Fe^{2+}. In this case, qualitative analysis based on Tanabe-Sugano diagrams allows unambiguous identification of the zero-phonon component at 1.22 eV and the 1.1 eV band with the transition $^3T_1(^3H) \rightarrow {}^5E(^5D)$. Therefore, from the spectroscopic data presented above, it follows that the transition $^3T_1(^3H) \rightarrow {}^5E(^5D)$ between the inner shells of the ion Fe^{2+} in ZnSe and CdTe forms similarly structured emission spectra, consisting of zero-phonon peak(s) and a broad band arising from interaction with the phonon subsystem. The spectral position of the zero-phonon peak (or center of gravity of the peak series) agrees with qualitative analysis within the framework of Tanabe-Sugano diagrams. Spectroscopic data on zero-phonon transitions involving states $^5T_2$ (^5D), ^5E (^5D), $^3T_1$ (^3H), obtained in this work and taken from works [28,31], are systematized in Table 1.

4. ROLE OF THE NEPHELAUXETIC EFFECT FE^{2+} IN CDTE AND CDTE

As follows from Fig. 2*a* and Table 1, in contrast to qualitative reasoning, quantitative analysis of spectroscopic data based on Tanabe-Sugano

Table 2. Energy values of transitions observed in the experiment for ZnSe:Fe and CdTe:Fe

	B, cm^{-1}	C, cm^{-1}	Dq, cm^{-1}	B_0, cm^{-1}	C_0, cm^{-1}	β_1
ZnSe:Fe	600(±15)	2733(±18)	300 [28]	917 [34]	4040 [34]	0.941
CdTe:Fe	500(±15)	2242(±29)	228 [28]	917 [34]	4040 [34]	0.778

diagrams for free ions Fe^{2+} encounters certain contradictions. The spectral position of zero-phonon lines for the transition corresponds to $^5T_2$ (^5D) → ^5E (^5D) and thus characterizes the crystal field magnitude. As seen from Table 1, the crystal field magnitude in ZnSe is 20–25 % higher than in CdTe. From the Tanabe-Sugano diagram in Fig. 2*a*, it immediately follows that in CdTe the transition $^3T1(^3H)$ → $^5E(^5D)$ should shift to the short-wavelength region compared to ZnSe. At the same time, experimental data shows the opposite trend – the corresponding line demonstrates a pronounced long-wavelength shift. We assume that this discrepancy illustrates an increase in the nephelauxetic effect during the transition from ZnSe to CdTe. Note that if we accept the decrease in energy of the state $^3T_1$ (^3H) relative to $^5E(^5D)$ and $^5T_2$ (^5D) due to the nephelauxetic effect, then the observed band for CdTe in the region of 0.9 eV falls exactly in the area where the emission of transition $^3T_1(^3H) \rightarrow {}^5T_2(^5D)$ should be registered.

According to crystal field theory, calculations of energy level splitting values can be performed with the crystal field splitting parameter Dq (ligand field splitting) for the matrix material and parameters determining electron-electron interaction [33]. In calculations, Slater integrals are used F_i, which, due to the complexity of performing initio calculations for ions in a crystal matrix that give results with spectroscopic accuracy, usually remain theoretical parameters and are determined experimentally [33]. Racah introduced new notations for Slater integrals, which are convenient to use as semi-empirical parameters when solving the problem [33],

$$B = \frac{9F^2 - 5F^4}{441}, \quad (2)$$

$$C = \frac{5F^4}{63}. \quad (3)$$

As noted above, the parameter Dq determines the distance between the lower levels ^5E and $^5T_2$ and therefore is unambiguously determined from experimental data. Parameters B and C for the free ion Fe^{2+} are given in reference books: $B_0 = 917$ cm^{-1}, $C_0 = 4040$ cm^{-1} [34]. When interpreting experimental data, phenomenological accounting for nephelauxetic effects can be accomplished by using Racah parameters B and C, whose values differ from those for free ions. In fact, this corresponds to an effective reduction in electron-electron repulsion. For an ion in the lattice, these parameters can also be calculated *ab initio* and are therefore convenient in developing and adapting rather complex modern theories.

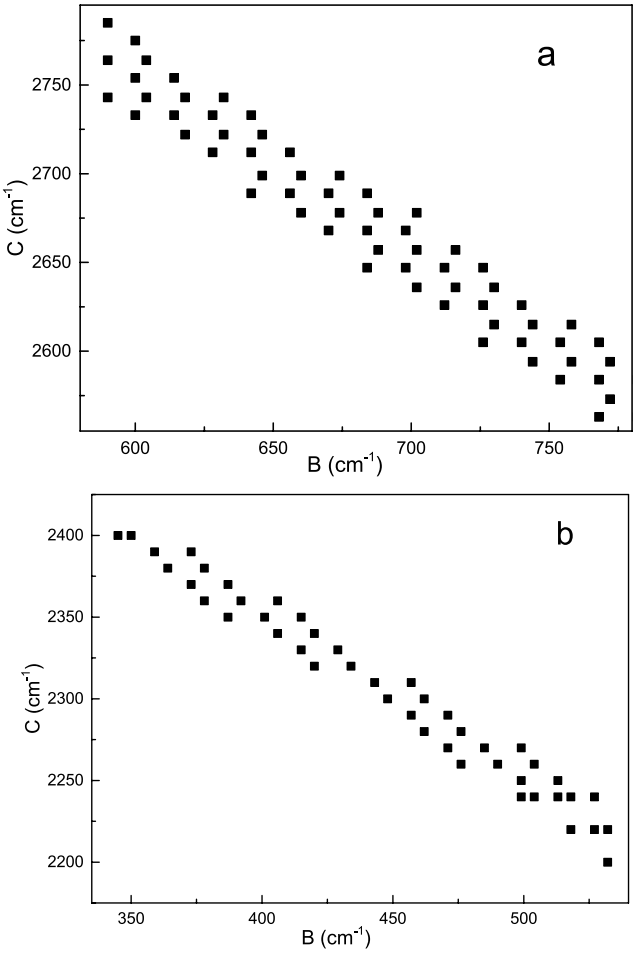

Fig. 6. Range of parameter values B and C , at which the desired value of 1.383 eV for level $^3T_1$ ZnSe:Fe (*a*) and 1.078 eV for level $^3T_1$ CdTe:Fe (*b*)

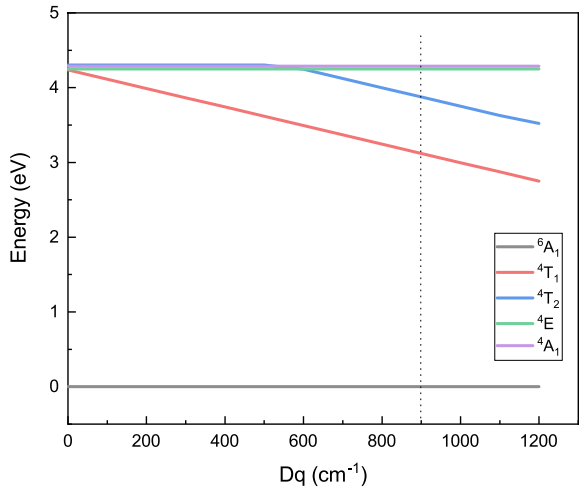

Fig. 7. Calculated dependence of energy splitting values in a tetrahedral crystal field on the field magnitude for ions Fe^{3+} (d^5). The dashed line shows the approximate position of the crystal field for the CdTe matrix

Our experimental data allowed us to refine the parameter values B and C for the ion Fe^{2+}, embedded in ZnSe and CdTe lattices. Fig. 6 shows the spread of acceptable parameter values B and C for our task, which give an energy shift between $^5E(^5D)$ and $^3T_1(^3H)$ of approximately 1.383 eV in ZnSe (Fig. 3) and approximately 1.078 eV in CdTe. As can be seen, the range of suitable value pairs in the case of ZnSe: $C = 2550 - 2800$ cm^{-1}, $B = 590 - 783$ cm^{-1}. These values were chosen according to the rule (pattern) of ratio $C/B = 4 - 4.5$ [26].

Furthermore, for iron group ions, a more significant decrease in parameter B than parameter C is expected, relative to free ion values. Consequently, as optimal parameters, one can choose $B = 600$ cm^{-1} (±15) and $C = 2733$ cm^{-1} (±18). The crystal field splitting magnitude $Dq = 228$ cm^{-1} cm in CdTe is somewhat lower than in ZnSe (see Table 1), due to differences in lattice parameters determining the crystal field magnitude, such as the ionic bond fraction. The range of suitable value pairs for Fe^{2+} in CdTe also differs from the free ion: $C = 2220 - 2280$ cm^{-1}, $B = 476 - 518$ cm^{-1} (Fig. 2*b*). We chose the average suitable Racah parameters and for the ion in CdTe: $B = 500$ (±18) cm^{-1}, $C = 2242$ (±29) cm^{-1}.

The determined Racah parameters (*B, C*) allowed us to further calculate the nephelauxetic effect magnitude, describing the degree of bond rigidity weakening in the ion (transition from ionic to covalent bonds). This effect (cloud expansion effect), most significant for *d*-transition elements, was very consistently considered by Jorgensen [8]. For these ions, there is an increase in *d*-orbital size due to their screening by lone electron pairs of ligands. The increase in nephelauxetic effect approximately corresponds to the growth of ligand-metal bond covalency.

As noted in the Introduction, several modified approaches to evaluating the nephelauxetic effect have recently emerged β_1 [7]. From relation (1), it follows that in ZnSe β_1(ZnSe)=0.941 (±0.04). A similar calculation for CdTe:Fe gives significantly lower values, indicating some weakening of the covalent bond: β_1(CdTe)= 0.778 (±0.08). All obtained parameters are shown in Table 2.

It should be noted that the increased role of the nephelauxetic effect in the case of the CdTe matrix is generally expected, as the higher value of Dq places ZnSe further right in the spectrochemical series of ligands [35], and the nephelauxetic effect typically manifests more strongly for weaker ligands [12]. However, this relationship is rather crude and often breaks down (see, for example, [36] and references therein), which is one manifestation of crystal field theory violations. A correct description of the nephelauxetic effect requires consideration of several factors, such as the influence of a specific ion's electron shell on the ligand electron shell, the dependence of the effect on the distance from the center to the ligand, as well as the role of dynamic and static correlation of electronic motion. To solve this problem, initio ligand field theory (*ab initio* ligand field theory, AILFT) [13] has been actively developed in recent years, combining ligand field theory methodology [14] and high-precision quantum chemistry methods that account for the multi-reference nature of electron wave functions involved in ion-ligand bonding, as well as dynamic correlation of ion and ligand electron motion. To the authors' knowledge, due to the complexity of the studied systems, such calculations for them are currently absent in the literature. Thus, the results obtained in this work can also serve to determine the accuracy and further development of modern theoretical approaches in the physics and chemistry of transition metal ions embedded in crystal matrices.

5. CONCLUSION

Thus, at helium temperatures, emission lines corresponding to transitions and $^3T_1$ (^5D) → ^5E (^5D) and $^3T_1$ (^5D) → $^5T_2$ (^5D) of the ion Fe^{2+} in the CdTe matrix were recorded. Taking into account the availability of comprehensive experimental data on the fine structure of the transition $^5T_2$ (^5D) → ^5E (^5D), this made it possible to conduct a comparative analysis of the nephelauxetic effect in the formation of the electronic spectrum of ions Fe^{2+} in CdTe and ZnSe matrices. These matrices have the same lattice type but differ in lattice constant value, crystal field magnitude, and the role of multi-electron corrections.

Calculations within the crystal field theory, based on the obtained experimental data and recent results from work [28], allowed to refine the semi-empirical Racah parameters for ions Fe^{2+} both in ZnSe — B = 600 cm^{-1}, C = 2733 cm^{-1}, and in CdTe — B = 500 cm^{-1}, C = 2242 cm^{-1}, as well as the magnitude of the nephelauxetic effect β_1 =0.941 for ions Fe^{2+} in ZnSe and β_1 =0.778 for Fe^{2+} in CdTe. We attribute the observed significant increase in the nephelauxetic effect in CdTe to the fact that in the case of ZnSe, the bond is more ionic in nature, which is expressed in a larger value of Dq. The tendency of the cubic CdTe matrix to form covalent bonds indicates that for ions placed in this matrix, one can expect more pronounced spectral effects related to the influence of multi-electron correlations. The obtained data, besides the possibility of direct use for quantitative description of the spectral properties of the studied centers, can serve to evaluate the accuracy of currently developing high- precision methods for describing the electronic properties of transition metal ions embedded in crystalline matrices.

FUNDING

This work was supported by the Russian Science Foundation under project No. 19- 79-30086.

APPENDIX. TANABE–SUGANO DIAGRAM FOR Fe^{3+} ION

In calculations, we used the values B = 1015 cm^{-1} and C = 4800 cm^{-1}. The crystal field splitting parameter for CdTe varies in the range 800–900 cm^{-1}. The calculation results are shown in Fig. 7. As follows from the diagram, the possible levels $^4T_1$ and $^4T_2$ lie significantly higher in energy ($^4T_1$ ~ 3.1 eV and $^4T_2$ ~ 4 eV), than the experimental values obtained and the results of similar calculations for Fe^{2+} ions presented in the main text of the work. Thus, we exclude the possibility of intracenter radiative transitions in Fe^{3+} in the luminescence spectra of the studied samples.

REFERENCES

1. A. E. Dormidonov, K. N. Firsov, E. M. Gavrishchuk et al., Appl. Phys. B 122, 211 (2016).
2. Y. Wang, T. T. Fernandez, N. Coluccelli et al., Opt. Express, 25, 25193 (2017).
3. S. Mirov, V. Fedorov, I. Moskalev et al., Journal of Luminescence, 133, 268 (2013).
4. J. Cook, M. Chazot, A. Kostogiannes et al., Opt. Mater. Express 12, 1555 (2022).
5. Y. Luo, M. Yin, L. Chen et al., Opt. Mater. Express 11, 2744 (2021).
6. A. I.Belogorokhov, M. I. Kulakov, V. A. Kremerman et al., Sov. Phys. JETP 67, 1184 (1988).
7. M. N. Sarychev, I. V. Zhevstovskikh, Yu. V. Korostelin, et al., JETP 163, 96 (2023).
8. A. M. Vorotynov, A. I. Pankrats, M. I. Kolkov, JETP 160, 670 (2021).
9. S. B. Mirov, I. S. Moskalev, S. Vasilyev et al., IEEE Journal of Selected Topics in Quantum Electronics 24, 1 (2018).
10. J. Shee, M. Loipersberger, D. Hait et al., J. Chem. Phys. 154, 194109 (2021).
11. K. Li, H. Lian, R. Van Deun et al., Dyes and Pigments 162, 214 (2019).
12. Chr. K. Jurgensen, Progress in Inorganic Chemistry 4, 73 (1962).
13. Molecular Electronic Structures of Transition Metal Complexes II. Structure and Bonding, ed. by D. Mingos, P. Day and J. Dahl, Springer, Berlin (2011).
14. B. N. Figgis and M. A. Hitchman, Ligand field theory and its applications, Wiley–VCH, New York (2000).
15. L. Lang, M. Atanasov and F. Neese, J. Phys. Chem. A 124, 1025 (2020).
16. E.-L. Andreici Etimie, N. M. Avram, and M. G. Brik, Opt. Mater.: X 16, 100188 (2022).
17. A. Suchocki, S. W. Biernacki, A. Kaminska et al., J. Lumin. 102-103, 571(2003).
18. K. P. O'Donnell, K. M. Lee, and G. D. Watkins, J.Phys.C: Solid State Phys. 16, 723 (1983).
19. J. W. Evans, T. R. Harris, B. R. Reddy et al., J. Lumin. 188, 541 (2017).

20. G. Roussos, H.-J. Schulz, M. Thiede, J. Lumin. 31-32, 409 (1984).

21. V. V. Fedorov, S. B. Mirov, A. Gallian et al., IEEE J. Quant. Electr. 42, 907 (2006).

22. A. Salem, E. Saion, N. Al-Hada et al., Appl. Sci. 6, 278 (2016).

23. E. E. Vogel, O. Mualin, M. A. de Orue et al., Physical Review B 50, 5231 (1994).

24. S. B. Mirov, V. V. Fedorov, D. Martyshkin et al., IEEE J. Selected Topics in Quan. Electron. 21, 1601719 (2015).

25. R. I. Avetisov, S. S. Balabanov, K. N. Firsov et al., J. Crystal Growth 491, 36 (2018).

26. A. Gladilin, S. Chentsov, O. Uvarov et al., J. Appl. Phys. 126, 015702 (2019).

27. M. P. Frolov, Yu. V. Korostelin, V. I. Kozlovsky, Ya. K. Skasyrsky, Opt. Lett. 44, 5453 (2019).

28. V. S. Krivobok, D. F. Aminev, E. E. Onishchenko et al., JETP Lett. 117, 344 (2023).

29. J. Peppers, V. V. Fedorov, and S.B. Mirov, Opt. Express 23, 4406 (2015).

30. R. Kernocker, K. Lischka, L. Palmetshofer et al., J. Crystal Growth 86, 625 (1988).

31. D. F. Aminev, A. A. Pruchkina, V. S. Krivobok et al., Opt. Mat. Express 11, 210 (2021).

32. V. S. Bagaev, V. S. Krivobok, E. E. Onishchenko et al., JETP 140, 929 (2011).

33. S. Sugano, Y. Tanabe, and H. Kamimura, Multiplets of Transition-Metal Ions in Crystals, Academic Press, New York (1970).

34. Y. Tanabe, S. Sugano, Journal of the Physical Society of Japan 9, 753 (1954).

35. C. E. Housecroft, A. G. Sharpe, Inorganic Chemistry (4th ed.), Prentice Hall, Hoboken (2012).

36. A. L. Tchougreff and R. Dronskowski, International Journal of Quantum Chemistry 109, 2606 (2009).